

High Porous Ceramic for Oil/Water Separation: Calcite as a Sintering Aid

Mohammed Abdulmunem Abdulhameed^{1*}, Mokdad Hayawi Rahman²,
Haider Nadhom Azziz¹

¹ Petroleum Engineering Department, University of Kerbala, Karbala 56001, Iraq

² Aeronautical Technical Engineering, Al-Farahidi University, Baghdad 10011, Iraq

* Corresponding author's e-mail: mohammed.abdulmunem@uokerbala.edu.iq

ABSTRACT

The effects of calcite (CaCO_3) as sintering aid on the preparation of local aluminum silicate microfiltration membranes were characterized in terms of morphology, thermal shrinkage behavior, porosity, permeation performance, and pure water permeate flux for the membrane. Material selection is based on availability and formability. In order to create a suspension, an organic solvent (N-methyl-2-pyrrolidone) and a polymer binder were added to a mixture of aluminum silicate and calcium carbonate. The coagulant bath consisted of water, and the suspension was extruded into a hollow fiber using a spinneret. The membrane precursor is subjected to high temperatures up to 1250 °C and this process called the sintering process gets strong hollow fiber with high mechanical stability. The addition of the CaCO_3 to the dispersion altered the structure of the resulting sintered membranes. The obtained finding demonstrates that carbon calcium addition to aluminum silicate has an affirmative on overall porosity in contrast to those made from purely natural aluminum silicate, as a result the aluminum silicate calcite ceramic microfiltration membrane, which had a high porosity of above 50%, shows the highest permeability of 35.8 ml $\text{m}^{-2}\cdot\text{s}^{-1}$ and above 97% oil rejection when operating at 0.15 MPa trans-membrane pressure in oil-in-water separation experiments. The results show that low-cost aluminum silicate-calcite component of ceramic membranes and the manufactured ceramic microfiltration membrane can handle emulsified oily wastewater.

Keywords: porous ceramic membrane; sintering aid; calcite.

INTRODUCTION

Recently significant attention in the application of membranes in separation processes due to the membrane processes is compact, further economical, and more efficient than the normal separation process (Saboyainsta and Maubois 2000). The process of membrane separation is assorted as nanofiltration, ultrafiltration, microfiltration, etc. Among the membranes process, microfiltration has the main variety of utilizations in many industries, due to the separation process of low energy consumption and high efficiency (Liu et al. 2016).

Features unique to the inorganic membrane, have placed it as a competitive alternative and a commodity sought for use in a variety of industries (Hubadillah et al. 2018). The membrane hollow fiber produced from ceramic material has

become widespread, not only because of their comparatively superior chemical and thermal resistance, as well as mechanical stability, but also due to their relatively higher surface/volume ratio in comparison to other geometric forms such as tubular and flat sheet (Sanchez et al. 2005).

Ceramic membranes are widely used in various industrial applications such as water treatment, food and beverage processing, pharmaceuticals, and biotechnology. However, the high cost of ceramic membranes has reduced their use in applications. In recent years, researchers have been working on developing low-cost ceramic membranes that can be used in various applications.

Traditionally, the majority of membranes prepared from ceramic material are made from costly metal oxides for instance zirconia, alumina, titania, or integration combination of these

oxides (Baig et al. 2022). Nevertheless, recently a tremendous effort has been made in membranes to evolve new highly porous ceramic from aluminum silicate clay (Sanchez et al. 2005; Liu et al. 2016). The advantages of aluminum silicate clay ($\text{Al}_2\text{Si}_2\text{O}_5$) include its low melting point, simplicity of processing, inertness, efficacy, and availability. The process of making an aluminum silicate membrane has been the subject of extensive study. Meanwhile, Bouzerara et al. have looked at making an aluminum silicate-based porous ceramic membrane using a slip-casting approach. Aluminum silicate is known to be abundant material and has a significant role in several manufacturing applications, for instance, high refractory properties and provides low plasticity (Indraratna, Korkitsuntornsan, and Nguyen 2020); it constitutes a preferable raw material for porous ceramics. In order to develop porous membranes with a low resistance to the fluid, it is vital to understand the fluid transport characteristics through the membrane. Until recently, many articles (Sadykov et al. 2022; Suwanmethanond et al. 2000; Bouzerara et al. 2006) have been concerned about the effect of sintering aid on its permselectivity.

Aluminum silicate ceramic hollow fiber membrane is a type of membrane technology used in water filtration and purification. It is made from kaolin clay, a naturally occurring mineral found in abundance around the world (Bouzerara et al. 2006). Aluminum silicate ceramic hollow fiber membranes are highly efficient at removing suspended solids, bacteria, viruses, and other contaminants from water (Bouzerara et al. 2006). The membrane is composed of a porous ceramic material with tiny pores that allow water to pass through while trapping contaminants on the surface, it has several advantages over other types of membranes. It is highly resistant to chemical attack, making it ideal for use in industrial applications where harsh chemicals are present. It also has excellent thermal stability and can withstand temperatures up to (260 °C) (Hubadillah et al. 2018). Additionally, the membrane has high porosity and permeability, allowing for efficient filtration of particles down to 0.1 microns in size.

The aluminum silicate ceramic hollow fiber membrane is also very cost-effective compared to other types of membranes (Yogarathinam et al. 2022). It requires minimal maintenance and can be used for many years without needing to be replaced or repaired. Additionally, it does not require pre-treatment or post-treatment steps like some other membranes do, making it an attractive option for those looking for an economical solution for their water filtration needs.

Numerous researchers have been looking at how to treat emulsified oily wastewater at a low cost utilizing porous ceramic membranes. This membrane, with an average pore size of 0.1 μm , was produced by (Bowen and Doneva 2000) using a one-step co-sintering procedure, and it showed strong rejection for oil and high steady-state permeability of $165 \text{ L m}^{-2}\cdot\text{h}^{-1}\cdot\text{bar}^{-1}$. The influence of various components on rejection and permeate flow was investigated by (Liu et al. 2016), who created membranes made of an inexpensive ceramic form of fly ash, quartz, and calcium carbonate. Microfiltration membranes made of aluminum silicate-based ceramics have the ability to efficiently separate oil and water which was studied, the authors investigated the relationship between membrane sintering temperatures, permeate flow, and rejection (Dong, Al-Jumaily, and Escobar 2018).

The objective of this work concerns the usefulness of the hollow fiber configuration for membrane made from ceramic material, thus, studying the possibility of aluminum silicate-calcite as a ceramic material for inexpensive porous ceramic hollow fiber membrane prepared via merged phase inversion /sintering technique. Two environmental issues were addressed in this work: emulsified oily wastewater treated using an aluminum silicate-calcite ceramic membrane, and using available local Iraqi aluminum silicate.

MATERIALS AND METHODS

Analysis of the raw materials

In this research, hollow fiber membranes were made using local aluminum silicate and

Table 1. Analysis of fluorescence XRD data reveals the chemical composition of aluminum silicate in weight percent

I.L	TiO ₂	F ₂ O ₃	CaO	K ₂ O	Na ₂ O	SiO ₂	Al ₂ O ₃	Oxides
18.73	0.22	0.23	0.32	0.95	1.12	45.00	33.43	Weight %

calcium carbonates. Table 1 shows kaolin's oxide weight percentages, revealing that this aluminum silicate is mostly made up of silica (SiO_2) and alumina (Al_2O_3). Dynamic Laser Beam Scattering (DLBS) was used to analyze the particle size distribution of aluminum silicate and calcium carbonate (Figure 1). The average particle size obtained with this technique was somewhere between 2.1 μm and 4.2 μm .

Membrane fabrication

The aluminum silicate-calcite was fabricated using the emerging phase inversion/sintering technique. Powdered aluminum silicate with an average particle size of 3–5 μm Doekhl, Iraq and PESf (Radel, USA) was dried to make ensure that no wetness was trapped. The Arlcel P135 was added to the organic solvent N-Methyl-2-pyrrolidone via a magnetic stirrer, before adding aluminum silicate powder. For 48 h the suspension was milled in a planetary by using different sizes of ball mill to ensure that the NMP, ceramic powder and Arlcel P135 were mixed well. Then PESf was used as a binder and milling continued for another 24 h. In order to finish the process of spinning the spinning suspension was treated for 15 min using a vacuum machine to remove any trapped air. The spinneret was used to extrude the ceramic dope by a syringe pump (KDS-100-CE, kdScientific, Holliston, MA). Tap water was used to solidify the hollow fiber which was lifted in H_2O overnight. The length of the hollow fibers was shortened to 30 cm before being sintered in the air in the high-temperature tubular furnace (MTI Corporation, Richmond, CA). The temperature for the sintering process was 1250 $^\circ\text{C}$.

Characterization

Observations of the surface morphologies of ceramic membranes were carried out with the assistance of a scanning electron microscope (NeoScope JCM-6000, manufactured in Japan). The sintering shrinkage curves of the membrane were measured using a horizontal dilatometer in the air between 50 and 1200 $^\circ\text{C}$, at a rate of 10 $^\circ\text{C}$ each minute (HSML-ODLT, Germany). The equation that was used to calculate the radial shrinkage percent, denoted by the letter "S," for sintered ceramic membranes is as follows:

$$S = \frac{L_0 - L}{L_0} \times 100\% \quad (1)$$

where: the diameters before and after sintering were denoted as L_0 and L , respectively. In accordance with Archimedes' principle, the porosity (P) of ceramic membranes was calculated using the following equation (2):

$$P = \frac{M_1 - M_2}{M_1 - M_3} \times 100\% \quad (2)$$

where: M_1 – the weight of samples when dry in the air;

M_3 – the weight of samples when saturated with water;

M_2 – the weight of samples when dry in water.

Permeate flux measurements and oil-in-water emulsion separation techniques

Figure 1 is a diagrammatic representation of a dead-end filtering instrument for removing oil from water emulsions and pure water permeates flux. Figure 1 depicts a schematic representation of a dead-end filtration device employed to separate oil-in-water emulsions and pure water permeate flux. The device comprises several key components, including a gas cylinder, a cylindrical stainless-steel liquid container, a membrane test holder, and a support frame shaped like a triangle. The ceramic membrane was first inserted into the membrane test holder and subsequently sealed on both sides using rubber rings. The liquid was then

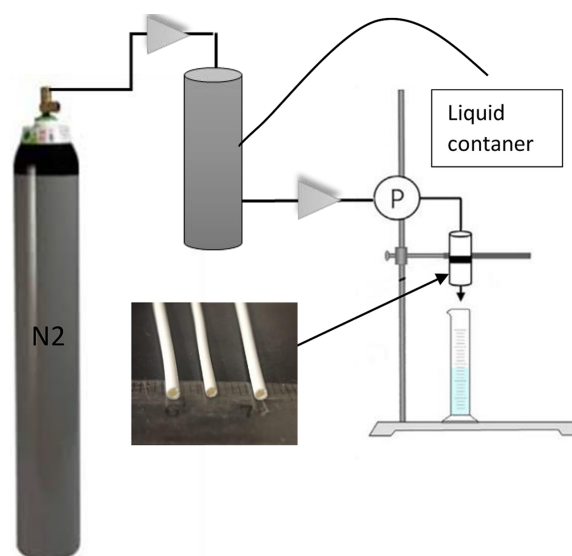


Figure 1. The measurement equipment for oil-in-water emulsion separation and pure water permeate flow

introduced into the holder under N_2 gas pressure, and it was compelled to pass through the ceramic membrane. To create a stable and homogeneous oil-in-water emulsion with a concentration of 250 mg/L, machine oil (GL-5, Qiangli) was dissolved in deionized water, and sodium dodecyl sulfate was added as a surfactant. The pressure that was applied to the transmembrane was in the range of 0.05–0.3 MPa, and the time it took for the separation process to complete was 50 minutes at each pressure point. At five-minute intervals, the oil concentration in the permeate was determined using the measurement. By measuring the absorbance using a UV–visible spectrophotometer (Shimadzu, Japan), it was possible to determine the amount of oil that was present in the permeate. According to the following formulae, the transmembrane flow (J , in $ml\ m^{-2}\cdot s^{-1}$) and the oil rejection (R) were calculated.

RESULTS AND DISCUSSION

Scanning electron microscope photos of the aluminum silicate-calcite and pure aluminum silicate hollow fibers were taken. Cross-sectional

structures of the pure aluminum silicate and the aluminum silicate-calcite are revealed in Figure 2a. In Figure 2, it is clear that the membrane has a consistent sponge-like structure throughout. The sponge-like structure appeared because of the gradual accumulation of precipitation that took place when the dispersion was brought into contact with the non-solvent (water) (Dong, Al-Jumaily, and Escobar 2018). The sintering process involves heating the aluminum silicate-calcite mixture at high temperatures, which causes the particles to become denser and form a solid mass. The morphological changes observed in Figures 2b and d can be attributed to this process. It has been found that the addition of calcite to the mixture can lead to an increase in the number of membrane pores, which can be beneficial for certain applications.

In Figure 3 the porosity of the aluminum silicate-calcite hollow fiber membrane compared to the pure aluminum silicate membrane can be seen. the obtained results indicate an inclination towards an increase in porosity upon the incorporation of $CaCO_3$ into the suspension dope. The underlying mechanism responsible for this observed phenomenon may be traced to the

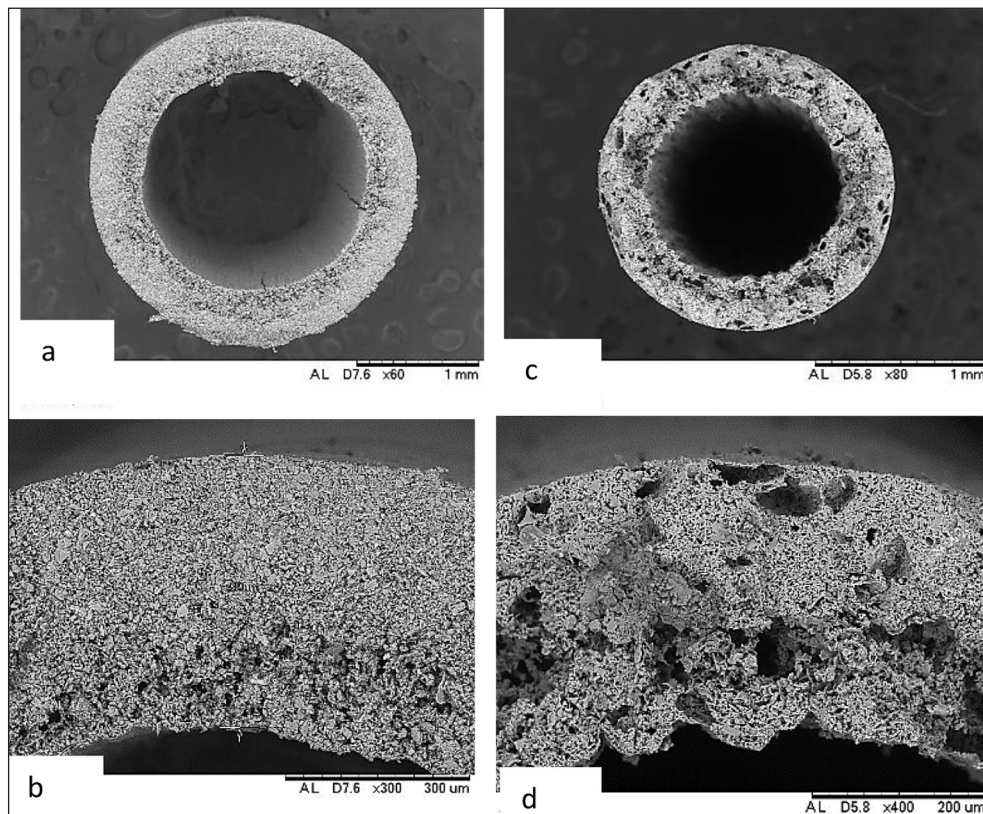


Figure 2 Cross-section of membranes: (a and b) membranes not including any $CaCO_3$, (c–d) membranes containing $CaCO_3$

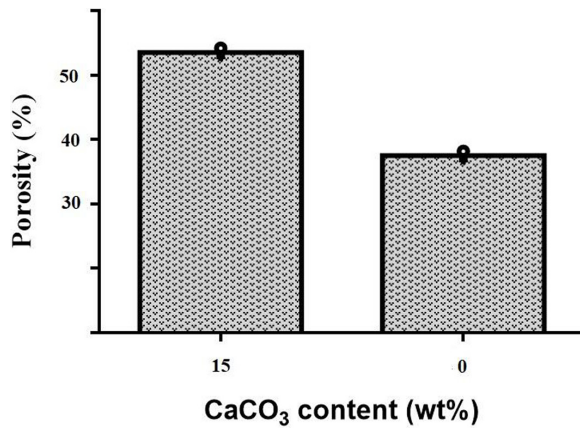


Figure 3. Porosity of hollow fiber membranes

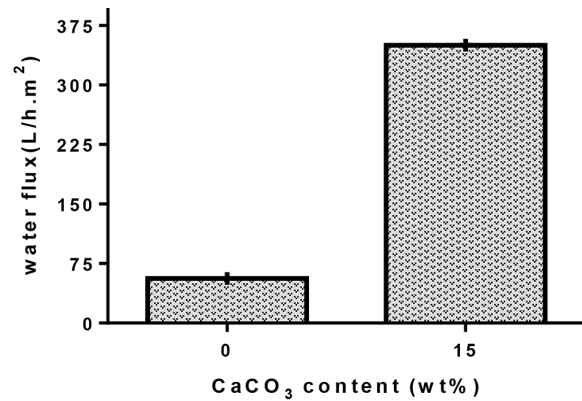


Figure 4. The distilled water flux of hollow fiber membranes

evaporation of calcite during high sintering temperatures. This process is believed to facilitate the arrangement of pores among the ceramic particles, consequently resulting in an augmentation of membrane porosity. This outcome is consistent with the densification of the membrane’s porous, sponge-like structure, as illustrated in Figure 2. Furthermore, a comparable trend of enhanced membrane porosity was also documented in a prior investigation conducted by Paiman et al. (2015) on Y-S zirconia hollow fiber membranes sintered within the temperature range of 1250 °C to 1400 °C.

Figure 4 illustrates the distilled water flux of aluminum silicate-calcite membrane compared with pure aluminum silicate membrane. As it was shown, the water flux through the membranes increases from 58 L·h⁻¹·m⁻² to 350 L·h⁻¹·m⁻² when adding CaCO₃ to the suspension dope. This is obtained because adding the CaCO₃ content promotes formation of space between the ceramic

particle after the sintering process in the fiber’s structure. It is important to point out that there is a vast gap in distilled water flux value for aluminum silicate-calcite compared to pure aluminum silicate, this can be explained based on the SEM image (Figure 2).

During the process of reactive sintering in the solid state, materials based on aluminum silicate are prepared. There are two basic mechanisms determining dimension shrinkage greater temperature causes ceramics to shrink due to a phenomenon known as sintering densification, whereas aluminum silicate growth causes samples to either expand or contract. A dynamic sintering curve may represent the interaction of two variables. The green rectangular samples with and without CaCO₃ are shown in sintering shrinkage curves in Figure 5. Addition of CaCO₃ has a major impact on the shrinkage behaviors, particularly at high temperatures. At this point, the CaCO₃-containing sample had a higher percentage of shrinkage and

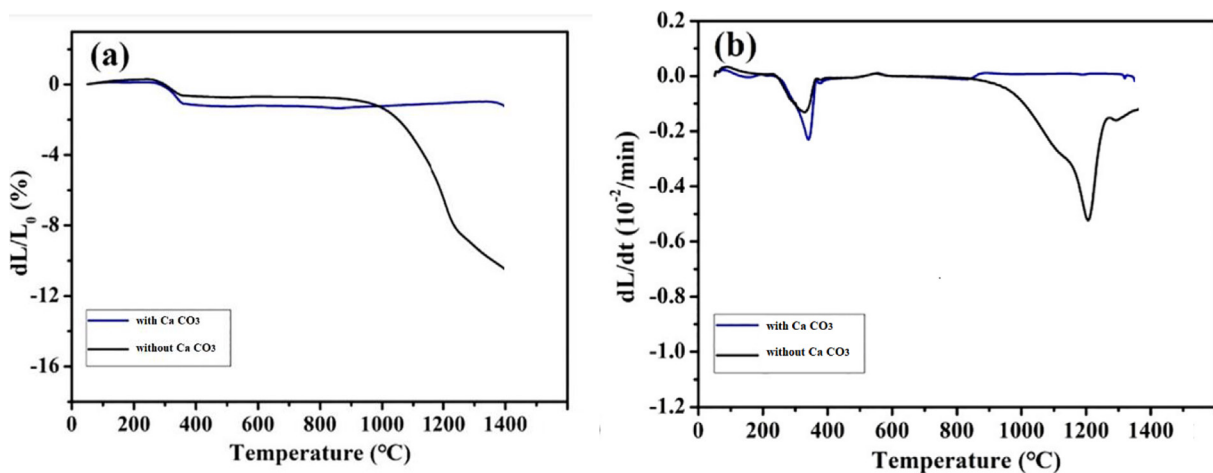


Figure 5. Curves of thermal contraction for green rectangular samples with and without CaCO₃ catalyst. (a) percentage of linear shrinkage; (b) rate of linear shrinkage

a faster shrinkage rate than the control sample. Following a plateau, the CaCO_3 -free sample shrinks noticeably, whereas the CaCO_3 -containing sample grows slowly. The large sintering densification behavior observed for the CaCO_3 -free sample corresponds to a shrinkage percentage of 7.7% in the temperature range of 800–1250 °C. The rapid initial shrinkage at temperatures below 1250 °C is followed by a gradual slowing of the densification shrinkage trend as temperatures rise (see Figure 5a). Minor expansion of around 0.4% from 850 to 1400 °C for the CaCO_3 sample corresponds to the mullitization reaction and the formation of mullite. As a result of the complete domination of high-temperature sintering densification behaviors after 1200 °C, the linear shrinkage percent and shrinkage rate dramatically rise for the two samples. There is a high danger of cracking and distortion in ceramic sintered bodies due to the considerable dimension shrinkage that occurs during sintering.

Figure 6 displays the relationship between sintering temperatures and porosity (in percentage) as well as average pore size. From 1100 to 1250 °C, both values rise before falling to 1250 °C. When the sintering temperature is raised from

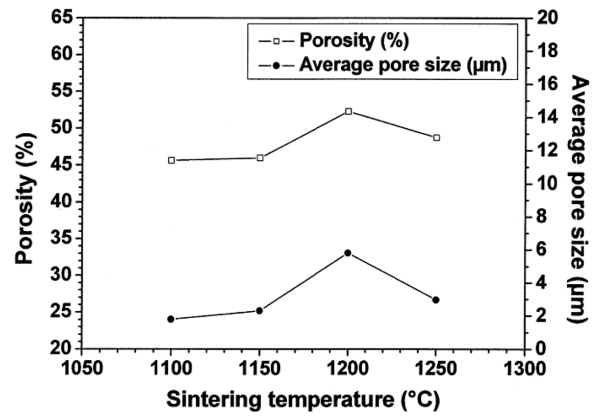


Figure 6. Porosity (%) and average pore size

1200 to 1250 °C, for instance, the porosity (percent) drops from 52 to around 49, and the average pore size drops from 6 to 3 µm. The improved sintering may account for the reduction in porosity (in percentage terms) and average pore size.

Small membrane holes contribute to the rejection of oil droplets, allowing the porous ceramic membrane to be used to treat emulsified oil. For the inexpensive and efficient treatment of emulsified oil, several low-cost membranes have been created to date. (Wang et al. 2022; Zou et al. 2019; Rashad

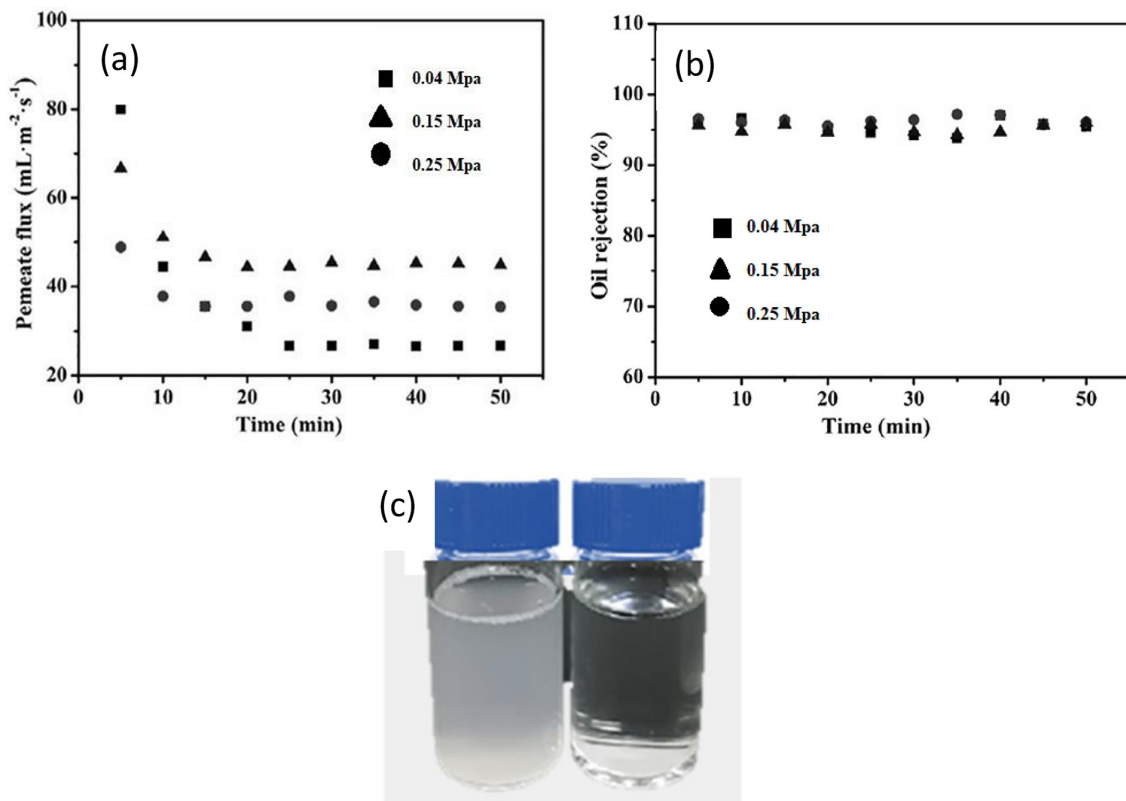


Figure 7. (a) Permeate flux, (b) porous aluminum silicate-calcite ceramic microfiltration membranes sintered at 1200 °C reject oil in an oil-in-water emulsion separation process running at 0.04, 0.15, and 0.25 kPa, (c) the visual contrast between the feed and the permeate

et al. 2021). The effectiveness of porous aluminum silicate-calcite ceramic membranes in separating oil-in-water emulsions while operating in a dead-end separation mode was studied and analyzed. This evaluation was carried out for the membrane that had CaCO_3 sintered at a temperature of 1200 °C. When the emulsion had been stable for at least 72 hours, it was filtered at three different transmembrane pressures of 0.04, 0.15, and 0.25 MPa. The oil content was measured to be $180 \text{ mg}\cdot\text{l}^{-1}$.

The time-dependent flow of permeate is shown in Figure 7b under a variety of different transmembrane pressures. It is clear to see that the process of membrane filtration may be broken up into two distinct steps. At the beginning of the filtration process, a considerable reduction in permeation flow occurs as a result of pore blockage and the accumulation of oil droplets on the membrane surface. Once a given amount of time has passed during the filtering process, a cake layer will have formed at the surface of the membrane, and the permeate flow will have reached a steady state. When there is a progressive rise in the transmembrane pressure, the permeation flux will also gradually increase. The time function of oil rejection is shown in Figure 7b at a variety of various transmembrane pressures. All of the oil rejections are greater than 96%, and there is no discernible difference detected between the various transmembrane pressures. This suggests that the membrane pores are sufficiently tiny to prevent oil droplets from passing through the ceramic membrane. The snapshot of an oil-in-water emulsion both before and after it was filtered is shown in Figure 7c. After filtering, as it was anticipated, the clean water solution was produced, which is in agreement with the outcome of the oil rejection. The membrane that was used in this study demonstrates a competitive edge over other low-cost ceramic membranes with symmetrical configurations, both in terms of its permeability and its oil rejection capabilities. The disclosed low-cost asymmetrical ceramic membrane has been shown to have somewhat greater permeability than the membrane that was developed for this study due to the significant structural advantage it has.

CONCLUSIONS

The highly porous aluminum silicate-calcite hollow fiber membrane was profitably fabricated via the phase inversion/sintering technique. By

adding the CaCO_3 content to the suspension dope, it was found that additives tend to increase the number of membrane pores, in turn influencing the qualities and performances of aluminum silicate-calcite hollow fiber membrane. On the basis of the findings obtained, it might be concluded the sintering aid e.g. (CaCO_3) has influenced the formation of the pore structure of the skin layer, resulting in a porous membrane structure with an overall porosity of 55% and excellent water flux of $350 \text{ L}/\text{m}^2\cdot\text{h}$. This preliminary data could develop a new and common vision for the preparation of porous membranes using aluminum silicate as the unexpansive ceramic material for application in removing oil from water separation and has an advantage over competitors in terms of permeability and oil rejection. Operating at a transmembrane pressure of 100 kPa allowed for an oil rejection rate that was more than 95% and a steady-state permeate flow that was measured at $35.8 \text{ mL}\cdot\text{m}^2\cdot\text{s}^{-1}$. The obtained findings demonstrate that the aluminum silicate-calcite component of low-cost ceramic membranes and the manufactured ceramic microfiltration membrane are both capable of being used in the process of treating emulsified oily wastewater.

Acknowledgments

The authors thankfully acknowledge the Assistance Service from Karbala university and Nippon Foundation.

REFERENCES

1. Baig, N., et al. 2022. Recent progress in microfiltration/ultrafiltration membranes for separation of oil and water emulsions. *The Chemical Record*, 22(7), e202100320.
2. Bouzerara, F., et al. 2006. Porous ceramic supports for membranes prepared from kaolin and dolomite mixtures. *Journal of the European Ceramic Society*, 26(9), 1663–1671.
3. Bowen, W.R., Doneva T.A. 2000. Atomic force microscopy studies of nanofiltration membranes: surface morphology, pore size distribution and adhesion. *Desalination*, 129(2), 163–172.
4. Dong, X., Al-Jumaily, A., Escobar I.C. 2018. Investigation of the use of a bio-derived solvent for non-solvent-induced phase separation (NIPS) fabrication of polysulfone membranes. *Membranes*, 8(2), 23.
5. Hubadillah, S.K., et al. 2018. Fabrications and

- applications of low cost ceramic membrane from kaolin: A comprehensive review. *Ceramics International*, 44(5), 4538–4560.
6. Indraratna, B., Korkitsuntornsan, W., Nguyen T.T. 2020. Influence of Kaolin content on the cyclic loading response of railway subgrade. *Transportation Geotechnics*, 22, 100319.
 7. Liu, Z., et al. 2016. Investigation of internal concentration polarization reduction in forward osmosis membrane using nano-CaCO₃ particles as sacrificial component. *Journal of Membrane Science*, 497, 485–493.
 8. Rashad, M., et al. 2021. A novel monolithic mullite microfiltration membrane for oil-in-water emulsion separation. *Journal of Membrane Science*, 620, 118857.
 9. Saboyainsta, L.V., Maubois J.-L. 2000. Current developments of microfiltration technology in the dairy industry. *Le Lait*, 80(6), 541–553.
 10. Sadykov, V.A., et al. 2022. Design of materials for solid oxide fuel cells, permselective membranes, and catalysts for biofuel transformation into syngas and hydrogen based on fundamental studies of their real structure, transport properties, and surface reactivity. *Current Opinion in Green and Sustainable Chemistry*, 33, 100558.
 11. Sanchez, C., et al. 2005. Applications of hybrid organic–inorganic nanocomposites. *Journal of Materials Chemistry*, 15(35–36), 3559–3592.
 12. Suwanmethanond, V., et al. 2000. Porous silicon carbide sintered substrates for high-temperature membranes. *Industrial & engineering chemistry research*, 39(9), 3264–3271.
 13. Wang, J., et al. 2022. Efficient oil-in-water emulsion separation in the low-cost bauxite ceramic membranes with hierarchically oriented straight pores. *Separation and Purification Technology*, 303, 122244.
 14. Yogarathinam, L.T., et al. 2022. Low-cost silica based ceramic supported thin film composite hollow fiber membrane from guinea corn husk ash for efficient removal of microplastic from aqueous solution. *Journal of hazardous materials*, 424, 127298.
 15. Zou, D., et al. 2019. One step co-sintering process for low-cost fly ash based ceramic microfiltration membrane in oil-in-water emulsion treatment. *Separation and Purification Technology*, 210, 511–520.